SICE Journal of Control, Measurement, and System Integration, Vol. 4, No. 1, pp. 037–042, January 2011

3D Beamforming Coupler for 2D Waveguides Using Dielectric Scatterer Array

Yasuaki MONNAI * and Hiroyuki SHINODA *

Abstract : We propose a novel directional antenna device that couples 2D guided microwaves with 3D radiated beams. It consists of a dielectric scatterer array aligned in two-dimensional periodicity on a planar surface-waveguide. Each scatterer radiates a portion of the incident guided wave in a location-dependent linear phase delay. Therefore, the directivity of the synthesized scattered wave is controllable by tuning the period of the scatterers. We derive a guideline to design the scatterer pattern for beamforming and verify it with numerical simulations. Since the proposed method works reversibly both on sending and receiving, microwave paths for wireless communication and sensing can be designed smartly.

Key Words : two-dimensional communication, waveguide, grating, antenna.

1. Introduction

Recently, the concept of Two-Dimensional Communication (2DC) has been proposed as a new class of wireless technology in which two-dimensional surface-waveguides are used for microwave transmission [1]. By confining microwave propagation two-dimensionally, high-efficient, leakage-secure, and interference-free wireless communications become available on the two-dimensional surface. Each device put on the surface can be wirelessly coupled to the waveguide using an evanescent field. By embedding those waveguides in various two-dimensional regions in our living environments, for example, desks, walls, floors, and even in clothes, many devices can easily be integrated into a wireless network.

Meanwhile, the 2DC has two drawbacks for its usage because of its principle. First, each device must not be apart from the waveguide surface more than only a few millimeters because the evanescent field decays rapidly along the normal direction to the surface. Of course it is this feature that enables the two-dimensional confinement of microwaves, however it restricts the spatial flexibility of the wireless communication at the same time. This restriction becomes harder when the wavelength gets shorter with higher frequencies. Second, microwave transmission over separated waveguides (for example, those embedded in a desk and a wall) is difficult. Unlike one-dimensional cables, the two-dimensional waveguides cannot be interconnected just by point-to-point contact at their ends. As a result, the use of 2DC has been limited only on a continuous two-dimensional region.

To solve these problems, the authors have recently proposed a novel directional antenna device which couples 2D guided microwaves with 3D radiated beams [2],[3]. They have demonstrated directional beam radiation from one-dimensional periodic array of dielectric scatterers on the surface of the waveguide. The beam direction can be tailored by tuning the scatterer period because each scatterer radiates a portion of the guided wave in a location-dependent phase delay. Since the proposed method works reversibly both on sending and receiving, it extends the wireless communication area of the 2DC smartly. This concept is an application of optical beam coupling techniques [4]–[7] to the microwave region. In the preceding works, the grating was one-dimensional and therefore the directivity was tailored only in the 2D cross sectional plane of the grating. This paper extends the grating periodicity into two-dimension in order to form a directional beam in the whole 3D space both in the polar angle direction and the azimuth angle direction as conceptually illustrated in Fig. 1. If the grating pattern is made tunable, the system works as a phased array with a quite thin and light body. Such a phased array also enables microwave sensing in indoor situations like passive radar detection of the locations of distributed wave sources such as RFID tags and wireless LAN nodes. Although we concentrate on microwave frequency in this paper, the proposed concept can also be applied to much higher frequencies including quasi-optical region by scaling the structure. However, this extension often requires significant modification in the structures at the same time due to the dispersive characteristics of the materials and that will be discussed elsewhere.

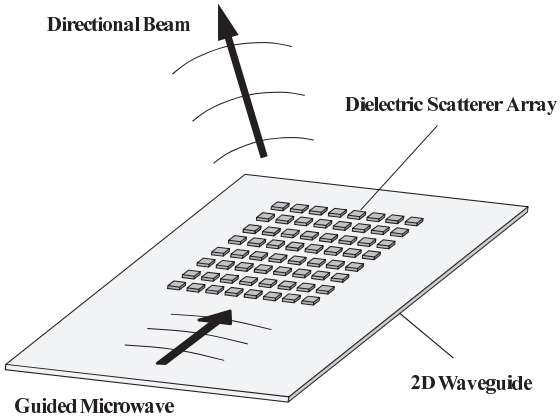

Fig. 1 Concept of the proposed beamforming coupler.

* Department of Information Physics and Computing, University of Tokyo, Tokyo, Japan
E-mail: monnai@alab.t.u-tokyo.ac.jp
(Received February 24, 2010)
(Revised September 9, 2010)

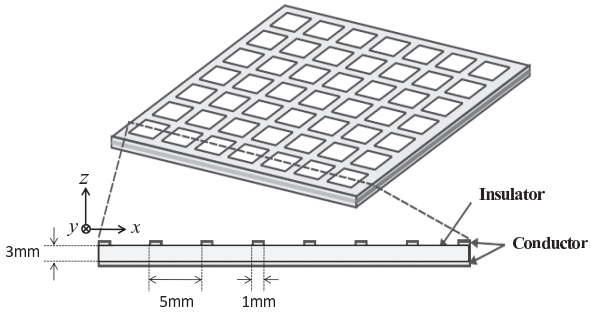

Fig. 2 Structure of the 2D waveguide.

2. Waveguide Scattering

The waveguide in consideration is a kind of 2D microstrip lines as illustrated in Fig. 2. It has a conductive mesh layer and a ground layer insulated by a dielectric substrate. The lattice period of the mesh is fabricated sufficiently shorter than the guided wavelength so that it works as an inductive surface on average [1]. In this paper, we consider a guided mode that travels one-dimensionally in the x-direction and has a uniform wavefront along the y-direction. The z-direction is defined perpendicular to the surface so that $z = 0$ corresponds to the waveguide surface. We define β_g $(= \omega/c)$ as the wavenumber of the guided wave in the x-direction, where ω and c are the angular frequency and the velocity of the guided microwave, respectively. When the microwave propagates inside the waveguide, a non-radiative evanescent field which also propagates in the x-direction and decays exponentially in the z-direction is formed on the waveguide surface.

The evanescent field is likely to be converted into radiation by scatterers. The scattering situation in consideration is illustrated in Fig. 3. The microwave propagates in the x-direction and has a uniform wavefront along the y-direction. The z-direction is defined perpendicular to the surface so that $z = 0$ corresponds to the waveguide surface. Scatterers can be implemented in various ways of perturbing the surface condition of the waveguide. For example, a local increase of the dielectric permittivity on the waveguide surface is known to work as a scatterer [5]. Although structural parameters of the scatterers such as shape, size, and dielectric permittivity are physically important, the optimization of them is out of interest in the paper (see [5]–[8] for more details.) Here we consider a simple thin dielectric block of half-wavelength long as a scatterer and concentrate on directivity control by tuning the array pattern. Each scatterer radiates a portion of the evanescent field in a location-dependent phase delay. Therefore, the directivity of the scattered field is controllable by tuning the spatial pattern of the scatterers. Far-field forming process with distributed wave sources is fundamentally described by the diffraction integral [9]. Assuming scalar waves for simplicity, the radiation from the aperture as illustrated in Fig. 3 is described as follows.

$$\psi(u,v,z) = A\int_S f(x,y)\,\frac{e^{j\beta_a R}}{R}\,g(u-x,v-y,z)\,dxdy \quad (1)$$

$$R = \sqrt{(u-x)^2+(v-y)^2+z^2} \quad (2)$$

where $\psi(u,v,z)$ is the complex amplitude at the observation point, A is an appropriate coefficient, S stands for the aperture region, $f(x,y)$ is the aperture function which is the complex

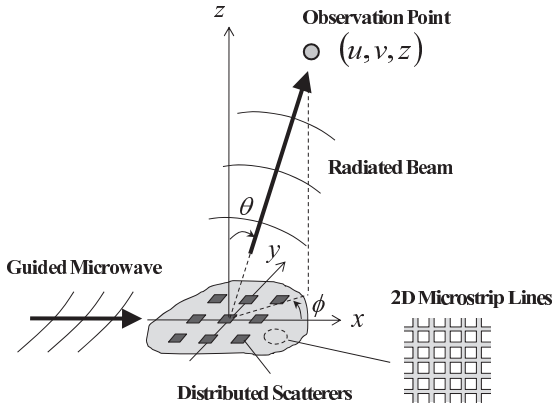

Fig. 3 Coordinate to describe the waveguide scattering.

weight for the distributed scatterers, R is the distance between the observation point and the distributed scatterers, β_a is the wavenumber of the radiated wave in the air, and $g(u-x,v-y,z)$ is a directivity of the radiation from $(x,y,0)$ toward (u,v,z). The goal of this paper is to show how to design $f(x,y)$ in order to obtain the desired directivity. Before proceeding into details, here we explain one simple guideline. In Fraunhofer's region where z is sufficiently far compared to the size of the aperture, (1) approximates to the following relation.

$$\psi(u,v,z) \simeq A\frac{e^{j\beta_a\left(z+\frac{u^2+v^2}{2z}\right)}}{z}g(u,v,z) \times\int_S f(x,y)\,e^{-j(ux+vy)/z}dxdy \quad (3)$$

As is well known from the diffraction theory, the integral in (3) is identical to the Fourier transform of $f(x,y)$. Therefore, the far-field pattern can be designed by tuning the complex weight $f(x,y)$ so that it becomes the inverse Fourier transform of the desired far-field pattern. For example, if $f(x,y)$ has a periodicity in the xy-plane, the radiation pattern also has a periodicity in the far-field, which is physically attributed to grating lobes. If the periodicity of $f(x,y)$ is small enough, the lobes other than the main one disappear, and strong directivity toward the main lobe will be obtained.

3. Directivity Forming

In this section, we discuss how the scatterer pattern is designed for a predefined beam-direction. A directional beam with a tilted wavefront is formed when each scatterer works in a linear phase delay. Therefore, we consider a 2D grating structure as shown in Fig. 4. The scatterers (in dark gray) are located at

$$x_{mn} = mp_x + nd_x \quad (4)$$

$$y_{mn} = np_y \quad (5)$$

where m and n are integers. For simplicity, each scattered wave is assumed to spread isotropically in the far-field. The far-field radiation pattern is calculated based on (1). Since the scatterers are located discretely, the superposition of each scattered wave is calculated by the following summation

$$\psi(u,v,z) = A\sum_{m=0}^{M-1}\sum_{n=0}^{N-1} f_{mn}\frac{e^{j\beta_a R_{mn}}}{R_{mn}} \quad (6)$$

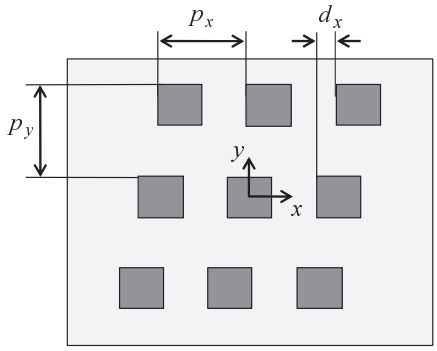

Fig. 4 Definition of the 2D periodic scatterer pattern. The scatterers (dark gray) consist of dielectric blocks.

where A is an appropriate coefficient, M and N are the numbers of the scatterers in the x and y directions, f_{mn} is a complex weight that represents scattering amplitude of the (m, n)-th scatterer, R_{mn} is the distance from each scatterer to the observation point, and β_a is the wavenumber of the radiated microwaves in the air. Considering the location-dependent amplitude decay and phase delay of the guided wave, f_{mn} is modeled as follows

$$f_{mn} = a_{mn} e^{j\beta_g (m p_x + n d_x)} \tag{7}$$

where a_{mn} represents the location-dependent amplitude decay and β_g is the wavenumber of the guided wave. The amplitude decay is attributed to both radiation-loss and material-loss, and results in the decrease of the aperture size (i.e. the number of the scatterers which contribute to the radiation). Substituting (7) into (6) and assuming that the observation point is sufficiently far from the scatterers, (6) approximates to

$$\begin{aligned}\psi(R,\theta,\phi) \simeq A \frac{e^{j\beta_a R}}{R} \sum_{m=0}^{M-1} \sum_{n=0}^{N-1} a_{mn} \\ \times e^{-jm\left(\beta_a p_x \sin\theta\cos\phi - \beta_g p_x\right)} \\ \times e^{-jn\left\{\beta_a\left(d_x \sin\theta\cos\phi + p_y \sin\theta\sin\phi\right) - \beta_g d_x\right\}}\end{aligned} \tag{8}$$

where (R, θ, ϕ) is the spherical coordinate of the observation point that relates to (u, v, z) by

$$u = R\sin\theta\cos\phi \tag{9}$$

$$v = R\sin\theta\sin\phi \tag{10}$$

$$z = R\cos\theta \tag{11}$$

(8) indicates that constructive interference occurs when the following conditions are satisfied.

$$\beta_a p_x \sin\theta\cos\phi - \beta_g p_x = 2\pi\mu \tag{12}$$

$$\beta_a\left(d_x \sin\theta\cos\phi + p_y \sin\theta\sin\phi\right) - \beta_g d_x = 2\pi\nu \tag{13}$$

where μ and ν are integers. Considering that β_g is larger than β_a for microstrip line-like waveguides, the main lobe is formed for $\mu = -1$ and $\nu = 0$. Conversely, in order to form a main lobe in the predefined direction in (θ_d, ϕ_d), the scatterer pattern, (p_x, d_x, p_y), needs to satisfy the following relations.

$$p_x = \frac{2\pi}{\beta_g - \beta_a \sin\theta_d \cos\phi_d} \tag{14}$$

$$\frac{d_x}{p_y} = \frac{\beta_a \sin\theta_d \sin\phi_d}{\beta_g - \beta_a \sin\theta_d \cos\phi_d} \tag{15}$$

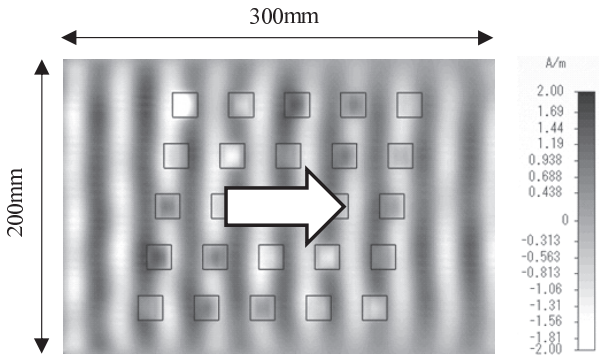

(a) Right above the Surface (z = 0.5 mm)

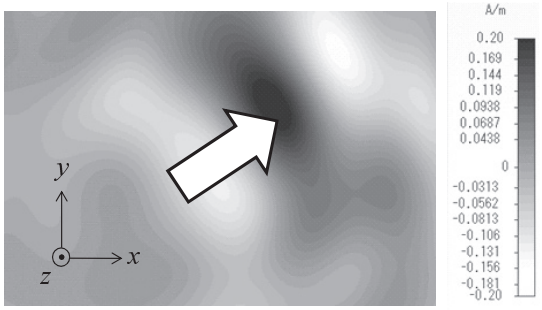

(b) Far from the Surface (z = 150 mm)

Fig. 5 Snapshots of the directivity forming process (H_y-component). The directivity was designed in $(\theta_d, \phi_d) = (20°, 45°)$. (a) The incident guided wave propagating in the x-direction was scattered by the scatterers (solid rectangulars) in a location-dependent phase delay. (b) As a result, a new wavefront in the other direction was formed in the far-field.

Note that d_x and p_y are not determined uniquely from the main lobe condition only. We determine these values based on the following consideration. In order to suppress side-lobes, it is required that (13) holds only for $\mu = -1$ and $\nu = 0$. This is satisfied when the following inequality holds.

$$\left(\beta_a + \beta_g\right) p_x < 4\pi \tag{16}$$

$$\beta_a \sqrt{d_x^2 + p_y^2} + \beta_g d_x \le 2\pi \tag{17}$$

In order to obtain sharp directivity, it is preferable that d_x and p_y are as large as possible within the range where (17) holds. Thus, combining the equal case of (17) with (15), we finally obtain (p_x, d_x, p_y).

As long as the aperture size is finite, the radiated beam is collimated only within a finite range, L, given by

$$L \simeq \frac{2D^2}{\lambda_a} \tag{18}$$

where D is the aperture size and $\lambda_a = 2\pi/\beta_a$ is the wavelengh in the air [10]. Thus, in order to transmit collimated microwaves over a long range, D needs to be increased with numbers of the scatterers. After passing through that range, the beam begins to diverge with a 3 dB beam-angle, θ_w, given as follows [11].

$$\theta_w \simeq \frac{\lambda_a}{D} \tag{19}$$

Assuming indoor wireless applications, D should be typically more than several wavelength. For example, a mouse-pad size

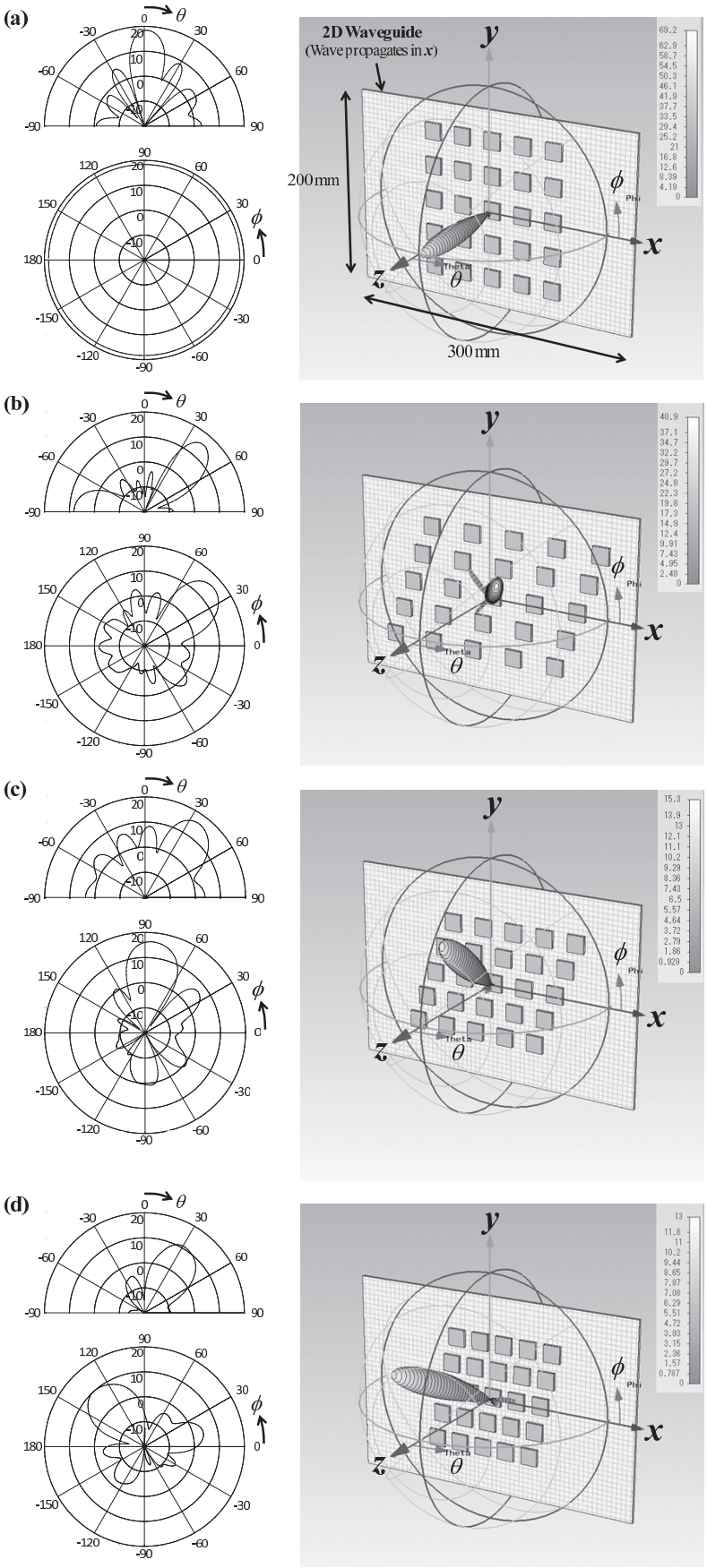

Fig. 6 Simulated beam steering by the 2D grating patterns where the beam direction, (θ_d, ϕ_d), was programmed in (a) (0°, 0°), (b) (40°, 45°), (c) (40°, 90°), and (d) (40°, 135°), respectively.

array of 200 mm × 200 mm works well at 5 GHz ($\lambda_a = 60$ mm) resulting in $L \simeq 1.3$ m and $\theta_w \simeq 17°$.

4. Simulations

In this section, we show several numerical simulation results of beamforming. The simulations were carried out with MW-Studio 2009 (CST) which is based on finite integration technique, and we investigated wave scattering at 5.5 GHz assuming microwave applications. We modeled the 2D microstrip lines with a lattice period of 5 mm and a line width of 1 mm as illustrated in Fig. 2. The insulator layer has a thickness of 3 mm and a relative permittivity of 2.7. Since the radiation-loss by the scatterer array was more dominant than the material-loss for the decay of the guided wave in our previous works [2],[3], we assumed loss-less materials in this simulation for simplicity.

First of all, we set no scatterers on the waveguide surface and excited a transverse magnetic guided wave from which we estimated the guided wavenumber, β_g, to be 190 m^{-1} at 5.5 GHz. Although it might be slightly modulated when some scatterers were put on the surface, we neglected that and used the above value as the normal wavenumber. We then aligned 5 × 5 pieces of scatterers on the waveguide surface according to (14)−(17). Each scatterer was modeled by a dielectric block with dimensions of 15 mm ×15 mm × 3 mm and a relative permittivity of 15. Figure 5 shows snapshots of the radiated field (y-component of the magnetic field) observed at (a) $z = 2$ mm (right above the surface) and (b) $z = 150$ mm (far from the surface) where the directivity was programmed in $(\theta_d, \phi_d) = (20°, 45°)$. As shown there, the incident guided wave propagating in the x-direction was scattered by the scatterers (solid rectangles) in a location-dependent linear phase delay in (a), and a new wavefront in the other direction was formed in the far-field in (b).

Next, we carried out a series of beamforming simulations around the z-axis. The results are shown in Fig. 6. On the right side of the figure, the scatterer patterns and the directivity plots (linear scale) are drawn in 3D graphics. At first, we set the beam direction in $\theta_d = 0°$ (vertical radiation) in Fig. 6 (a). Subsequently, we set the polar angle in $\theta_d = 40°$ and swept the azimuth angle as $\phi_d = -135°, -90°, -45°, 45°, 90°, 135°$. Here we show the results for (b) 45°, (c) 90°, and (d) 135° in Fig. 6. As expected, the beam direction was controllable by tuning the scatterer pattern. Although only the cases for $\phi_d > 0°$ are shown here, we confirmed that beams for $\phi_d < 0°$ were also formed by mirrored scatterer arrays with respect to the y-axis. On the left side of the figure, the detail profiles of the directivity are plotted in dB scale for $-90° \le \theta \le 90°$ (at $\phi = \phi_d$) and $-180° \le \phi \le 180°$ (at $\theta = \theta_d$). The errors of the simulated beam direction from the predefined beam direction, $(\Delta\theta, \Delta\phi)$, were (a) (2°, indefinable), (b) (2°, −5°), (c) (−4°, −4°), and (d) (−9°, −3°), respectively. In order to reduce the errors, more precise phase tuning of each scattered wave is required because the wavenumber β_g is slightly modulated when the scatterers are aligned on the waveguide surface. The simulated antenna gain and the 3 dB beam angle in the polar angle direction and the azimuth angle direction were (a) 18.4 dB, 16.8°, indefinable, (b) 16.1 dB, 18°, 23°, (c) 15.3 dB, 23°, 27°, and (d) 11.1 dB, 28°, 33°, respectively. The radiation efficiency calculated by integrating the Poynting vector over the simulated space was (a) 16%, (b) 30%, (c) 25%, and (d) 20%, respectively. The remaining power was transmitted to the other end of the waveguide not being radiated by the scatterers. By putting more scatterers both in the x- and y-directions, the aperture size is enlarged and sharper directivity is attained according to (19). The increase of the scatterer number also leads to the rise of the amount of radiation.

5. Conclusion

We have proposed a novel antenna device which couples 2D-guided microwaves with 3D-radiated beams. It is based on waveguide scattering from 2D periodic scatterers on the waveguide surface. We explained how to form a directional beam in the 3D space by tuning the 2D grating pattern. The feasibility of the proposed method was verified with numerical simulations. The next work is to implement an electronically tunable grating pattern which is the key to construct a phased array system. Since it leads to a phased array radar with a quite thin and light body compared to the conventional systems, there are many promising applications with respect to wireless communications and microwave sensing. Candidates for the tunable scatterers include the array of semiconductor switches like FETs or more optical materials such as liquid crystals.

Acknowledgement

The research was partly supported by the Grant-in-Aid for the JSPS Fellows (22-4238), National Institute of Information and Communications Technology (NICT) 13701, and the Murata Science Foundation.

References

[1] H. Shinoda, Y. Makino, N. Yamahira, and H. Itai: Surface sensor network using inductive signal transmission layer, *Proc. INSS 2007*, pp. 201–206, 2007.

[2] Y. Monnai and H. Shinoda: Converting 2D microwave into 3D beam using dielectric grating antenna, *Proc. INSS 2009*, pp. 183–187, 2009.

[3] Y. Monnai and H. Shinoda: Microwave beam coupler between two-dimensional communication medium and surrounding space using dielectric grating, *Trans. IEICE*, Vol. J92-C, No. 12, pp.797–805, 2009 (in Japanese).

[4] M. L. Dakss, L. Kuhn, P. F. Heidrich, and B. A. Scott: Grating coupler for efficient excitation of optical guided waves in thin films, *Appl. Phys. Lett.*, Vol. 16, No. 12, pp. 523–525, 1970.

[5] H. Nishihara, M. Haruna, and T. Suhara: *Optical Integrated Circuits*, McGraw-Hill Professional, 1989.

[6] T. Tamir and S.T. Peng: Analysis and design of grating couplers, *Appl. Phys. A*, Vol. 14, No. 3, pp. 235–254, 1977.

[7] K. Ogawa, W.S.C. Chang, B. L. Sopori, and F. J. Rosenbaum: A theoretical analysis of etched grating couplers for integrated optics, *IEEE J. Quantum Electron.*, Vol. QE-9, No. 1, pp. 29–42, 1973.

[8] F.K. Schwering and S.T. Peng: Design of dielectric grating antennas for millimeter-wave applications, *IEEE Trans. Microwave Theory Tech.*, Vol. 31, No. 2, pp. 199–209, 1983.

[9] M. Born and E. Wolf: *Principles of Optics*, Pergamon Press, 1970.

[10] A.D. Yaghjian: An overview of near-field antenna measurements, *IEEE Trans. Antennas Propagat.*, Vol. 34, No. 1, pp. 30–45, 1986.

[11] R.J. Mailloux: Phased array theory and technology, *Proc. IEEE*, Vol. 70, No. 3, pp. 246–291, 1982.

Yasuaki Monnai (Student Member)

He received his B.S. degree in mathematical engineering and information physics and M.S. degree in information physics and computing from the University of Tokyo, Japan, in 2008 and 2010, respectively. He is currently working toward the Ph.D. degree at the same university. He is a Research Fellow of the Japan Society for the Promotion of Science. He is a guest scientist at the Institute of Nanostructure Technologies and Analytics, University of Kassel, Germany. His research interest includes controlling electromagnetic wave propagation by designing the structure or morphology of transmission systems and applying them to wireless communication, measurements, and human-machine interfaces. He is a student member of IEICE and IEEE.

Hiroyuki Shinoda (Member)

He received the B.S. degree in applied physics, the M.S. degree in information physics, and the Ph.D. degree in electrical engineering from the University of Tokyo, Japan, in 1988, 1990, and 1995, respectively. He was a Lecturer from 1995 and an Associate Professor from 1997, both in the Department of Electrical and Electronic Engineering, Tokyo University of Agriculture and Technology, Japan. He was a visiting researcher at the University of California, Berkeley in 1999. From 2000, he is an Associate Professor in the Graduate School of Information Science and Technology, University of Tokyo. His research interest includes information physics, tactile/haptic interfaces, sensor systems and devices, sensor networks, two-dimensional communication, human interfaces, and optical/acoustic measurement. He was a board member of SICE in 2008 and 2009, and is a member of IEEJ, RSJ, VRSJ, JSME and IEEE.